Accelerated Publications

The 2.1 Å Structure of *Torpedo californica* Creatine Kinase Complexed with the ADP-Mg^{2+}−NO_3^-−Creatine Transition-State Analogue Complex[†,‡]

Sushmita D. Lahiri,[§] Pan-Fen Wang,[||] Patricia C. Babbitt,[⊥] Michael J. McLeish,[||] George L. Kenyon,[||] and Karen N. Allen*[,§]

Department of Physiology and Biophysics, Boston University School of Medicine, Boston, Massachusetts 02155, Department of Medicinal Chemistry, College of Pharmacy, University of Michigan, Ann Arbor, Michigan 48109-1065, and Departments of Biopharmaceutical Sciences and Pharmaceutical Chemistry, School of Pharmacy, University of California, San Francisco, California 94143-0446

Received August 15, 2002; Revised Manuscript Received September 12, 2002

ABSTRACT: Creatine kinase (CK) catalyzes the reversible conversion of creatine and ATP to phosphocreatine and ADP, thereby helping maintain energy homeostasis in the cell. Here we report the first X-ray structure of CK bound to a transition-state analogue complex (CK−TSAC). Cocrystallization of the enzyme from *Torpedo californica* (TcCK) with ADP-Mg^{2+}, nitrate, and creatine yielded a homodimer, one monomer of which was liganded to a TSAC complex while the second monomer was bound to ADP-Mg^{2+} alone. The structures of both monomers were determined to 2.1 Å resolution. The creatine is located with the guanidino nitrogen cis to the methyl group positioned to perform in-line attack at the γ-phosphate of ATP-Mg^{2+}, while the ADP-Mg^{2+} is in a conformation similar to that found in the TSAC-bound structure of the homologue arginine kinase (AK). Three ligands to Mg^{2+} are contributed by ADP and nitrate and three by ordered water molecules. The most striking difference between the substrate-bound and TSAC-bound structures is the movement of two loops, comprising residues 60−70 and residues 323−332. In the TSAC-bound structure, both loops move into the active site, resulting in the positioning of two hydrophobic residues (one from each loop), Ile69 and Val325, near the methyl group of creatine. This apparently provides a specificity pocket for optimal creatine binding as this interaction is missing in the AK structure. In addition, the active site of the transition-state analogue complex is completely occluded from solvent, unlike the ADP-Mg^{2+}-bound monomer and the unliganded structures reported previously.

Creatine kinase (CK, EC 2.7.3.2), a member of the guanidino kinase superfamily, catalyzes the reversible phosphorylation of creatine (Cr), transferring the phosphate group from ATP-Mg^{2+} and forming phosphocreatine (PCr) and ADP-Mg^{2+} (*1*, *2*). Phosphorylated guanidino compounds (phosphagens), such as phosphocreatine (PCr), are considered to be reservoirs of "high-energy phosphate" which are able to supply ATP on demand. Consequently, CK plays a significant role in energy homeostasis in cells with intermittently high energy requirements, by shuttling energy between different cellular compartments (*1*, *3*). As may be expected for an enzyme playing such a crucial role in energy homeostasis, CK is a highly conserved enzyme with a sequence that is ∼60% identical across all species.

Considerable efforts have been made in the past 30 years to understand the mechanism of CK. Much of the early biochemical characterization was carried out on the cytosolic isozyme from rabbit muscle and is summarized in a review by Kenyon and Reed (*4*). More recently, these studies have been augmented by the analysis of site-directed mutants confirming that cysteine, histidine, and glutamic acid residues are important for binding and catalysis (*5*−*8*). However, none of these studies provided conclusive evidence of a specific mechanism, although it is clear that phosphoryl group transfer between ATP and creatine takes place with in-line attack and inversion of the γ-phosphate configuration (*9*). Five structures of CK are currently available in the Protein Data Bank (*10*−*14*). Consistent with their significant level of sequence similarity, all the reported structures of CKs are highly homologous. Each monomer consists of two domains, a smaller N-terminal domain of ∼100 residues and a larger

[†] This work was supported by U.S. Public Health Service Grant AR17323 (to G.L.K.) and also in part by GM16099 (K.N.A.). Use of the Advanced Photon Source was supported by the U.S. Department of Energy, Basic Energy Sciences, Office of Science, under Contract W-31-109-Eng-38. Use of the BioCARS Sector 14 was supported by the National Institutes of Health, National Center for Research Resources, under Grant RR07707.

[‡] The coordinates of the refined structure have been deposited with the Protein Data Bank (entry 1N16).

* To whom correspondence should be addressed: Department of Physiology and Biophysics, Boston University School of Medicine, 715 Albany St., Boston, MA 02118-2394. Phone: (617) 638-4398. Fax: (617) 638-4273. E-mail: allen@med-xtal.bu.edu.

[§] Boston University School of Medicine.

[||] University of Michigan.

[⊥] University of California.

10.1021/bi026655p CCC: $22.00
Published on Web 11/19/2002

C-terminal domain of ~280 residues. The ATP binding site is located in the cleft between the two domains. None of the X-ray structures show CK bound to either creatine or a transition-state analogue.

To date, the most useful information about guanidino kinases has been obtained from the structure of arginine kinase (AK) complexed with a transition-state analogue complex (AK−TSAC) (*15*). The sequence of AK, the CK homologue found in arthropods and other invertebrates, is ~45% identical and 55% similar with those of the various CKs, and the gross structure of the AK−TSAC complex is very similar to the structures reported for CK. However, it was clear that there is considerable movement of some residues as substrates bind. In particular, the AK−TSAC structure suggests that a flexible loop, probably comprising residues 322−332, can be expected to close over the creatine binding site. Further, in CK, there is a second flexible loop consisting of residues 60−70 which has been hypothesized to move upon substrate binding (*16*, *17*). The analogous region of AK contains a much shorter loop. Sequence alignments show that all CKs contain an additional PGHP motif in this region. Given that many of the determinants of specificity that will distinguish CK from AK and the other guanidino kinases are likely to reside on those loops (*15*), a high-resolution structure of a CK−ligand complex could prove to be invaluable to understanding the specificity of CK and, potentially, of all guanidino kinases.

Herein, we report the first crystal structures of CK from *Torpedo californica* (TcCK) bound to a substrate, ADP-Mg^{2+}, and to a transition-state analogue complex comprising ADP-Mg^{2+}, NO_3^-, and creatine (*18*). The two structures have allowed the identification of the residues involved in substrate−TSAC binding as well as analysis of the conformational changes associated with substrate binding. In addition, comparison with the AK−TSAC structure has helped us recognize some of the residues involved in substrate specificity.

MATERIALS AND METHODS

Purification, Characterization, and Crystallization. TcCK was cloned and expressed as reported previously (*19*). The native molecular weight of TcCK was determined by both size-exclusion chromatography and native gel electrophoresis. The former was carried out using a 1.6 cm × 94 cm Sephacryl S-200 column, employing 50 mM sodium phosphate buffer (pH 7.0) containing 150 mM NaCl. Using a calibration curve of standards (Amersham Pharmacia), the native molecular weight of TcCK was estimated to be 83 600. In the latter method, native Tris/glycine gels were run at acrylamide concentrations of 5, 7.5, 10, and 12.5%. A calibration kit for native electrophoresis (Amersham Pharmacia) was used to generate a standard curve (Ferguson plot) as described elsewhere (*20*). Using this method, the native molecular weight of TcCK was estimated to be 82 000. Given that the molecular weight of the TcCK monomer is 42 796 (*19*), these results indicate that TcCK is a dimer in its native state.

The purified protein (15 mg/mL), dissolved in 1 mM Hepes buffer (pH 7.5), was crystallized in the presence of 4 mM ADP, 5 mM $MgCl_2$, 20 mM creatine, and 50 mM KNO_3 (*21*, *22*). The protein transition-state analogue complex was screened for crystallization by sparse matrix screening (*23*) with Crystal Screen I and II (Hampton Research). Conditions obtained from this screen were further optimized to 0.01 M nickel chloride hexahydrate, 0.1 M Tris (pH 8.0), and 16% (w/v) PEG 2000, yielding large square crystals with overall dimensions of 0.4 mm × 0.4 mm × 0.4 mm.

Table 1: Summarized Crystallographic and Refinement Statistics

unit cell dimensions (Å)	$a = 70.6$, $b = 87.2$, $c = 127.6$
space group	$P2_12_12_1$
X-ray source	APS 14-BM-C
wavelength (Å)	1.000
resolution range (Å)	50−2.1
no. of total/unique reflections	456811/47094
completeness (%)[a]	92.5 (87.4)
$I/\sigma(I)$	21.9 (7.5)
R_{merge}[b] (%)	0.043 (0.2)
refinement statistics	
ligands	2 Mg^{2+}, 2 ADP, 1 NO_3, 1 creatine, 145 H_2O
no. of protein atoms/asymmetric unit	5884
no. of reflections (working set/free set)	38379/4303
R_{work}[c]/R_{free}[d] (%)	23.9/27.8
average *B*-factor (Å^2)	
average of all amino acid residues	28.5
average of main chain atoms	29.0
Mg^{2+} (2 total)	37.4
ADP (2 total)	23.5
creatine (1 total)	24.0
NO_3^- (1 total)	30.5
Luzzati coordinate error (Å)	0.29
rmsd	
bond lengths (Å)	0.01
angles (deg)	1.68
dihedrals (deg)	23.66
impropers (deg)	1.12

[a] The completeness of the outermost shell (2.17−2.09 Å) is shown in parentheses. [b] $R_{merge} = \sum_{hkl}\sum_i|I_{hkl,i} - \langle I_{hkl}\rangle I|/\sum_{hkl}\sum_i|I_{hkl,i}|$, where $\langle I_{hkl}\rangle$ is the mean intensity of the multiple $I_{hkl,i}$ observations for symmetry-related reflections. [c] $R_{work} = \sum_{hkl}|F_o - F_c|/\sum_{hkl}|F_o|$. [d] $R_{free} = \sum_{hkl}\sum_T|F_o - F_c|/\sum_{hkl}|F_o|$, where the test set, T, includes 10% of the data.

Diffraction Data Collection. Crystals were flash-frozen for data collection in 100% Paratone-N (Hampton Research). Diffraction data were collected to 2.1 Å resolution at the Argonne National Laboratory (beamline BM 14C) using a CCD Q4 detector. Data were measured and scaled using DENZO and SCALEPACK (*24*). Data collection statistics are summarized in Table 1. The crystals are orthorhombic, crystallizing in space group $P2_12_12_1$ with the following unit cell dimensions: $a = 70.6$ Å, $b = 87.2$ Å, and $c = 127.6$ Å. The unit cell volume is consistent with the presence of a dimer in the asymmetric unit (*25*).

Phase Determination, Refinement, and the Final Model. The phase problem was solved using the molecular replacement method. A monomer of chicken brain CK (84% level of sequence similarity, PDB entry 1QH4) with side chains mutated to Ala was used as a starting model for rotation and translation function searches using the program aMoRe in the CCP4 program suite (*26*), yielding a correlation coefficient of 49.2% and an *R*-factor of 40.5% for the correct solution which was comprised of two monomers. The model obtained from aMoRe was further refined using CNS (*27*). The N-terminal (residues 1−100) and the C-terminal (residues 101−381) domains were allowed to move independently in rigid body refinement, yielding initial R_{cryst} and R_{free} values of 44.8 and 45.8%, respectively.

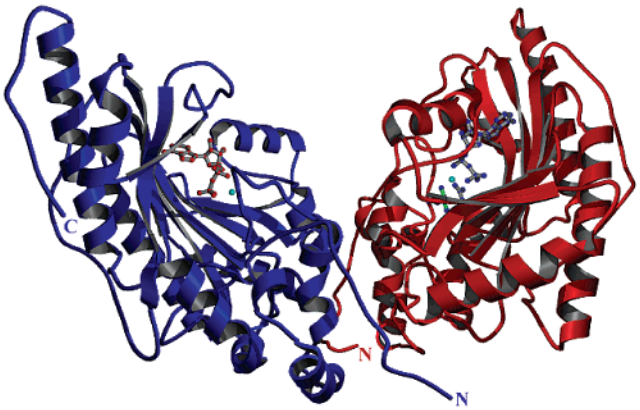

FIGURE 1: Ribbon diagram of the CK dimer. The E−ADP structure is depicted in red and the CK−TSAC structure in blue. The ligands are depicted as balls and sticks, and the Mg^{2+} ion is depicted as a cyan sphere.

The model from rigid body refinement was improved by performing successive rounds of manual rebuilding using the molecular graphics program O (*28*) followed by minimization and simulated annealing in CNS with data to 2.1 Å. To avoid any model bias, ligand molecules were added when R_{free} was <29%. The model creatine structure was obtained from Woordenboek Organische Chemie, and those of ADP-Mg^{2+} and nitrate were from the structure of the AK−TSAC complex. At this stage in refinement, waters were also added (145 waters total in the asymmetric unit which includes two monomers). N-Terminal residues (residues 1−7 and 1−11 in the two monomers) did not have clear electron density, and were excluded from the model. The final model comprises two monomers with 369 and 374 amino acids, 145 waters, two Mg^{2+} ions, two ADP molecules, one NO_3^-, and one creatine molecule, with an R_{free} of 27% and an R_{cryst} of 24% (Table 1). Analysis of the Ramachandran plot showed that 93.0% of the residues fall in the most favored regions, with 7.0% in the additionally allowed regions, and no residues fall in the generously allowed or disallowed regions, as defined by PROCHECK (*29*).

RESULTS AND DISCUSSION

Overall Structure and Fold. CK is prevalent in the tissues of *T. californica*, presumably as a result of the high energy requirements of electric discharge. The TcCK sequence was considerably similar (nearly 90%) to the sequences of both rabbit muscle and human muscle CK, and 55% similar to that of AK. The crystals were grown in the presence of the components of a transition-state analogue complex (ADP-Mg^{2+}−NO_3^-−creatine) (*30*). In the complex, the γ-phosphate of ATP is replaced with a nitrate ion, thereby mimicking a planar exploded metaphosphate-like transition state (*31*). The enzyme crystallizes with two monomers in the asymmetric unit. The overall structure of TcCK consists of a smaller N-terminal helical domain (residues 1−100) and a larger C-terminal α/β domain (residues 120−380) (Figure 1). The overall fold of the structure of TcCK is considerably similar to those of the other known CKs, i.e., rabbit muscle (*10*), chicken brain (*11*), bovine kidney (*14*), chicken mitochondrial (*32*), and human mitochondrial (*12*) as well as that of AK (*15*). Although the N- and C-terminal domains of ligand-bound TcCK can, individually, be overlaid successfully with the corresponding domain of the other known CK structures, the two domains have come closer together, indicating that the ligand-bound TcCK is a "closed" structure relative to the unliganded "open" structures. In addition, the two highly flexible loops (residues 60−70 and 323−332), which had been hypothesized to move during substrate binding and catalysis, are also more ordered in this structure with *B*-factors between 23 and 39% (compared to the average main chain *B*-factor of 29%). The two monomers in the asymmetric unit interact in a fashion similar to that of the known CK dimers (mitochondrial and brain) This result is consistent with the evidence from gel filtration (see Materials and Methods). Taken together, the data indicate that in the structure presented herein the two monomers in the asymmetric unit correspond to a physiological dimer.

Enzyme−Substrate and Enzyme−Transition-State Complex. Although the crystals were grown under known concentrations favoring formation of the transition-state complex, only one monomer had the transition-state analogue complex bound (CK−TSAC). The other monomer contained only the substrate ADP-Mg^{2+} bound in the active site (E−ADP). This dichotomy proved to be advantageous to us, since it provided a unique view of both the enzyme−substrate and enzyme−transition-state analogue complex forms.

The ADP-Mg^{2+} molecule in the E−ADP complex can almost be superimposed with the ADP-Mg^{2+} of the CK−TSAC form, as well as with the ADP-Mg^{2+} of the AK−TSAC structure, indicating a lack of strain or distortion on this substrate during catalysis. In the structure reported herein, the strong density surrounding all ligands bound to the active site (seen at the 4σ contour level in a $2F_o - F_c$ electron density map; see Figure 2a) and the low *B*-factors of the ligands (*23*−*26*) indicate that the density corresponds to well-ordered ligands of the enzyme. The adenine base in ADP in both E−ADP and CK−TSAC complexes is in the anti conformation with respect to the ribose ring, as had been predicted by earlier nuclear magnetic resonance experiments (*33*). The residues lining the ADP binding site that hold the nucleotide are almost identical in the two monomers. The adenosine rings are positioned by stacking interactions and hydrogen bonds to histidines, the main chain, and a few tightly bound water molecules. The histidines within 3.0 Å of the adenine ring include His296, which makes a stacking interaction with the six-membered ring of adenine, and His191, which forms a hydrogen bond to the 2′-hydroxyl group of the ribose ring along with the main chain N from Gly223. The mutation of His296 causes a substantial decrease in the specific activity of the enzyme (*6*), consistent with the importance of its role in stabilizing the position of the adenosine moiety. Other interactions with the adenosine group are made through three water molecules that bridge the side chain carboxylate group of Asp335 and main chain carbonyl oxygens of Arg292 and Ile188.

The remaining portion of the active site includes the nucleotide phosphate binding site (α, β, and γ) and the creatine binding site (*34*). The phosphate binding pocket is formed by a concentration of positive charges, comprised chiefly of five highly conserved arginine residues (Arg130, Arg132, Arg236, Arg292, and Arg320) and the Mg^{2+}. The arginines interact directly with the nonbridging phosphate oxygens, through monodentate interactions (from Arg132 Nη1 and Arg292 Nϵ to the β-phosphate) and bidentate interactions (Arg236 with the β-phosphate and nitrate oxy-

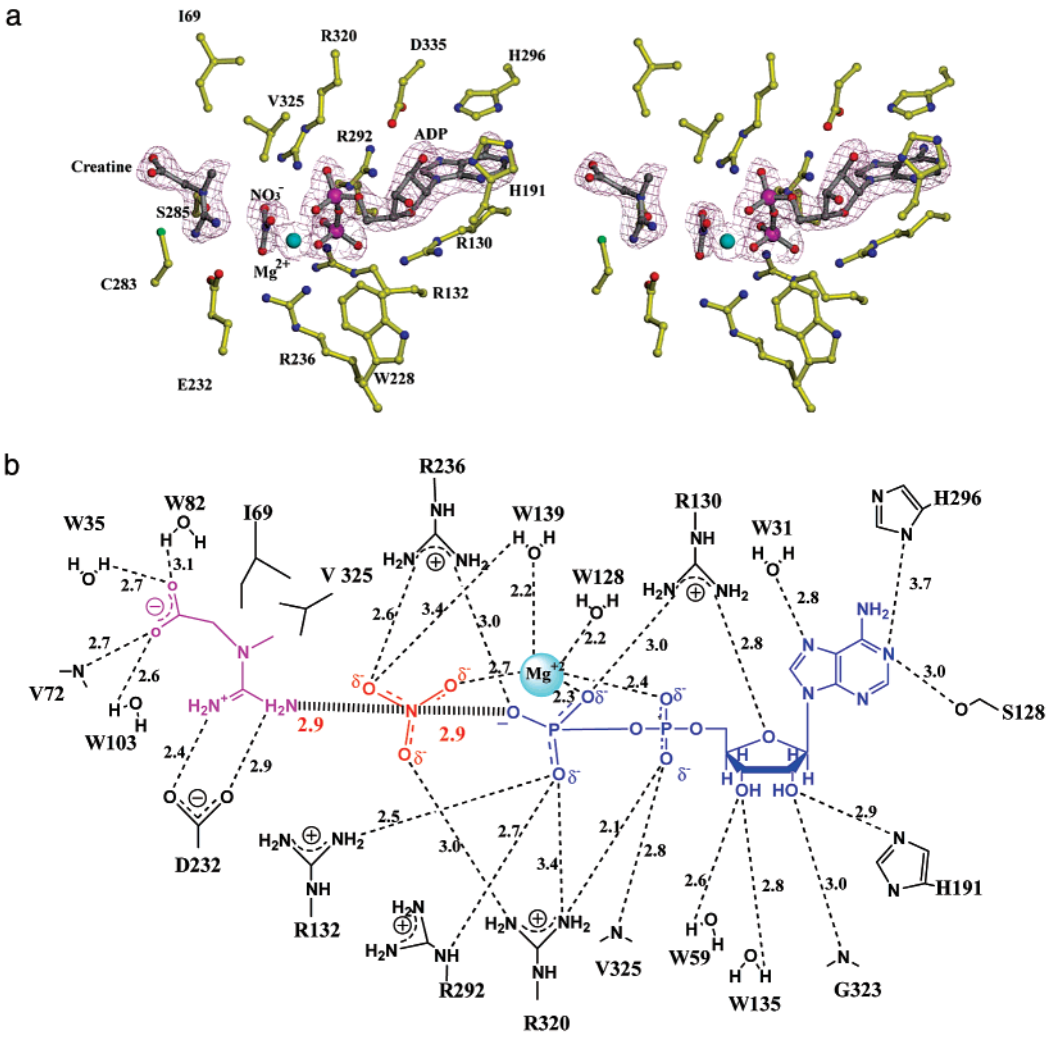

FIGURE 2: (a) Stereoview of the active site residues of the CK-TSAC structure. The ligands are shown as ball-and-stick models. The ligand atoms are shown in gray and the protein residues in yellow. The $2F_o - F_c$ electron density map contoured at 4σ is depicted as pink cages. (b) Chemdraw figure of the active site of the CK−TSAC structure (distances in angstroms).

gens, Arg320 with the α-phosphate and nitrate oxygens, and Arg130 with a *β*-phosphate oxygen and the ring oxygen of the ribose). In addition to stabilizing the negatively charged phosphate groups, these interactions will apparently help position the ATP-Mg^{2+} in line with creatine for nucleophilic attack. The arginine ligands are in the same position in both the CK−TSAC and E−ADP structures, with the exception of Arg320. In the E−ADP structure, this residue interacts with the nonbridged oxygen of the α-phosphate only. In the CK−TSAC complex (Figure 2b), Arg320 changes ligand geometry to bidentate with an additional hydrogen bond formed to the oxygen of the nitrate group. It is of interest that Arg320 is located at the base of one of the flexible loops (residues 323−332, Figures 3 and 4) and thus may be involved in conformational switching (*17*). Positively charged residues surrounding the phosphate portion of the ATP-Mg^{2+} will assist in the desolvation and binding of the highly negatively charged complex in the relatively water poor environment of the active site. Thus, the charged enzymatic side chains replace solvent interactions with ATP-Mg^{2+}. Two further interactions with phosphate involve the main chain nitrogen of Val325 and Mg^{2+}. In addition, Trp228 (*35*) does not interact directly with the substrate but forms part of the lining of the nucleotide binding pocket. Mutating this residue disrupts substrate binding and results in the complete inactivation of the enzyme (*17*).

The Mg^{2+} ion has an octahedral coordination geometry involving three nonbridging oxygens from two phosphates of the ADP group, one nitrate oxygen, and three water molecules (Wat127, Wat128, and Wat139), as seen in the CK−TSAC complex. The α-phosphoryl oxygen that is liganded to the Mg^{2+} ion is the pro-*R* oxygen (*36*, *37*), also seen in the AK−TSAC structure. The Mg^{2+} ligands in each of the two CK monomers are essentially superimposable, with a water molecule replacing the nitrate in the E−ADP complex. The coordination geometry of the metal ion and the stereochemical configuration of the metal nucleotide complex were predicted by elegant EPR studies on the Mn^{2+}-substituted protein, bound to ADP-Mg^{2+}, formate, and creatine, more than 20 years ago (*38*).

Work by Herschlag and Jencks (*39*) has demonstrated that, in solution, the effect of Mg^{2+} and Ca^{2+} ions on the reaction of *p*-nitrophenyl phosphate dianion with substituted pyridines is *not* consistent with a role for the metal ion in changing the character of the transition state. Thus, there is no chemical evidence for electrophilic catalysis in which the metal interacts with the nonbonded phosphoryl oxygen atoms to polarize the bond and enhance the electrophilicity of the

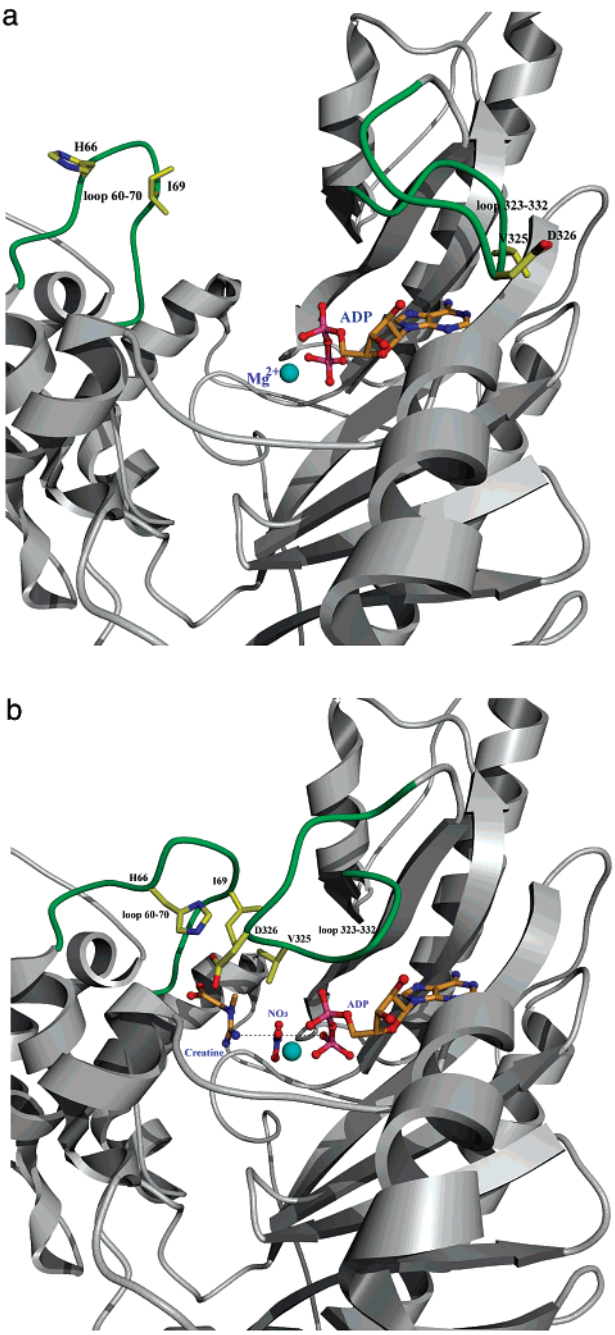

FIGURE 3: Diagram of the (a) E−ADP and (b) CK−TSAC structures. The backbone chain is shown as a gray ribbon diagram. The ligands and side chains are shown as ball-and-stick models. The Mg^{2+} is shown in cyan. The two mobile loops are colored green.

phosphorus. However, the binding of Mg^{2+} to the ADP anion should serve to decrease its basicity and stabilize the leaving group.

The nitrate ion mimics the γ-phosphoryl group being transferred in the intermediate state between a dissociated metaphosphate and a pentavalent form (the "exploded" transition state) (*31*). In this complex, unlike the γ-phosphoryl group in the true transition state, the nitrate is not constrained by partial bonds to the β-phosphate and the creatine guanidinium group. Nonetheless, the plane of the anion is perpendicular to a line connecting the guanidine nitrogen of creatine and the oxygen of the β-phosphate group, passing through the center of the nitrate moiety (Figure 3b).

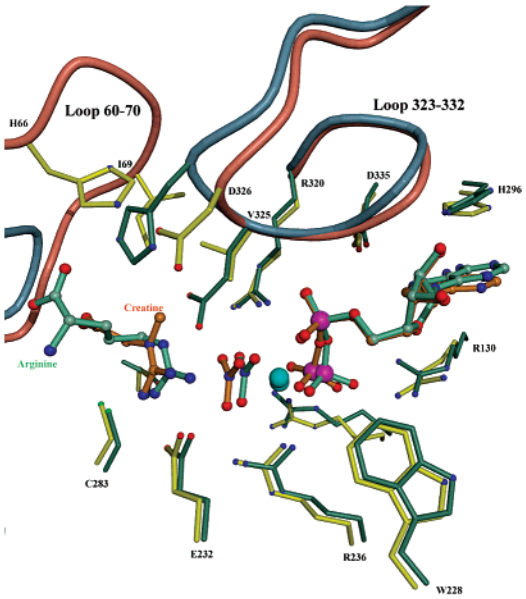

FIGURE 4: Overlay of the active site residues of the CK−TSAC (yellow bonds and pink loops) and the AK−TSAC structures (gray bonds and loops) (*15*). The ligands are depicted as balls and sticks for CK (tan) and AK (gray). Residue numbers correspond to CK.

The ligands to the nitrate oxygen atoms include the Mg^{2+} ion, Arg236, Wat139 (also a Mg^{2+} ligand), and Arg320, which is a part of the flexible loop (residues 323−332). Arg320 has moved compared to its position in the CK−ADP complex. Anions such as nitrate interact only weakly with divalent metal ions, and this association is made possible by the stabilizing interactions with the positively charged arginines located on either side of the nitrate anion.

The transition-state complex structure of CK affords the first view of the creatine binding pocket in this enzyme (Figures 2a and 3b). It also allows the comparison of the creatine binding site with the arginine binding site in AK, thereby helping to identify the residues involved in attaining substrate specificity (Figure 4). When the creatine and AK−TSAC structures are compared, the positions of the guanidinium groups of creatine and arginine do not differ significantly. In addition, the structural basis for the stereoselective phosphorylation of the guanidino nitrogen cis to the methyl group of creatine, deduced earlier by studies employing the conformationally restricted analogue, cyclocreatine (*40*, *41*), is now apparent.

Glu232 forms a bidentate salt bridge with the creatine guanidino group, analogous to Glu225 in AK. The similarity between the two binding sites ends here. Whereas the arginine binding site is relatively large to accommodate the substrate, the creatine binding site is much smaller. Unlike the carboxylate group of arginine which forms hydrogen bonds with the main chain nitrogens of loop residues Gly64, Val65, and Gly66, and the side chain nitrogen (Nϵ2) of His315, the carboxylate group of creatine is only stabilized by a hydrogen bond between the creatine carboxylate group and the main chain N of Val72. All other interactions are via water molecules positioned by protein side chains. In CK, the creatine methyl group is evidently used as a "specificity handle". To achieve this, the enzyme has customized an active site such that two hydrophobic residues, Ile69 and Val325, form a "pocket" for the methyl group. In the arginine binding site, the hydrophobic residues are

replaced with the negatively charged Glu314 which forms a hydrogen bond to Nϵ of the substrate. This is a striking difference between the arginine and creatine binding sites. Interestingly, the residues that form the greasy pocket in CK are contributed by the two mobile loops of the structure and are not part of the active site in the E−ADP complex (Figure 3a). Thus, at some point during the reaction mechanism, either upon creatine binding or further along the reaction coordinate when the transition state is achieved, the two loops close down on the active site and form the creatine binding pocket (Figure 3b). Substrate specificity studies have shown that replacement of the creatine methyl group with the more bulky ethyl group or a smaller hydrogen reduces the binding affinity of the substrate by 11- or 43-fold, respectively (*42*). Thus, the enzyme uses a sieving mechanism to achieve selectivity toward potential substrates.

In addition to forming a salt bridge to stabilize the positively charged guanidinium group, Glu232 is in the correct position to act as a general base catalyst to remove a proton from the nucleophilic nitrogen of the creatine guanidino group. Evidence to support this role comes from site-directed mutagenesis studies which show that replacement of this group with even a conservative mutation to aspartate results in a 500-fold loss of activity (*8*). The other important residue in the vicinity is Cys283 (Figure 2) seen interacting with the non-nucleophilic η-nitrogen of creatine (i.e., the nitrogen trans to the methyl group). This residue has been demonstrated to have a relatively low pK_a value of 5.4; i.e., for optimal binding of creatine, Cys283 should be in the thiolate anion form (*43*). Mutation of Cys283 to Met led to total loss of activity, while mutation to Ser produces a drastically reduced V_{max} ($\sim$100 times) and significantly ($>$10-fold) increased K_m for creatine (*43*). The nearby Ser285 interacts with Cys283, lowering its pK_a and stabilizing the thiolate form (*43*). It should be also noted that, when creatine binds, both Cys283 and Glu232 move closer to the phosphate binding pocket.

Cys283 keeps creatine anchored and positions it precisely for nucleophilic attack on the γ-phosphorus of ATP-Mg^{2+}. The precise positioning of the substrate in the Michaelis complex through formation of complementary surface charges in the CK−TSAC complex suggests that the activity of CK depends greatly on catalysis by approximation. This hypothesis is consistent with the recent study by Borders et al. (*44*), who used fluorescence quenching in the rabbit muscle enzyme to determine the constant that describes the dissociation of the CK−TSAC complex into its individual components (3×10^{-10} M^3). The aggregate affinities for the transition-state analogue components are high despite the unfavorable entropic contribution for formation of a quaternary complex, which is consistent with a role for the enzyme in bringing together and orienting substrates. In AK, a similar mode of binding is also seen to assist in the precise positioning of the substrates. Thus, it appears that catalysis by approximation is a major mode of catalysis utilized by all guanidino kinases.

Change in Conformation upon Binding. The overall structure of the E−ADP-bound form of CK was different from that of the CK−TSAC form. The two domains of the E−ADP monomer have moved as rigid bodies with respect to those of the CK−TSAC monomer. In addition, the two flexible loops comprising the nucleotide and creatine binding sites undergo a significant conformational change. The residues on loop 323−332 make contact with the α- and β-phosphates of the ADP, whereas residues from loop 60−70 and loop 323−332 (Ile69 and Val325) form the creatine binding pocket. His66, part of the conserved PGHP motif of CK found in loop 60−70, has been reported to be important for the catalytic reaction. It was suggested that this histidine moves significantly following substrate binding, possibly contributing to the electrostatic environment of the active site, although it did not act as an acid−base catalyst (*16*, *45*). Our structure clearly shows that His66 interacts with the carboxyl group of Asp326 from loop 323−332, effectively "latching" the two loops into the "closed" conformation. Completely "unlatching" the loops with the D326A mutation produces a loss in activity of approximately 3 orders of magnitude (*8*).

It is interesting to note that His66 of TcCK overlays in three-dimensional space with His316 of AK (Figure 4). However, the latter histidine is located on the opposite active site loop (residues 309−319) and, rather than forming a latch, instead forms a hydrogen bond with the arginine substrate. It should also be noted that the shorter loop in the AK−TSAC structure is unlikely to move significantly upon substrate binding by comparison to loop 60−70 of the CK−TSAC structure (Figure 4).

Half-Site Reactivity (Negative Cooperativity). The crystallographic asymmetric unit observed herein contains two monomers that are not identical in either their conformation or ligand binding state. The biological dimer is built from one each of these monomers plus one symmetry mate. Thus, each biological dimer is comprised of one monomer in the E−ADP state and one in the CK−TSAC state. This is puzzling, given the fact that the concentration of ligand in the transition-state complex was in excess of that of the protein and was well above the K_i of the TSAC. Examination of the crystal contacts for the two monomers shows that there are no constraints on the conformation of the mobile loops imposed by crystallization. It is possible that the observed structure could be the result of negative cooperativity between monomers in the biological dimer. Negative cooperativity has previously been observed in rabbit muscle CK in experiments measuring the modification of the active site Cys by 5′,5″-dithio(bis-2-nitrobenzoic acid) (DTNB) in the presence of the TSAC (*46*). The data from this study were consistent with a kinetic mechanism in which the presence of the transition-state analogue causes the two monomers to have different tertiary structures and behave differently toward the modifying agent (*47*). Certainly, it is obvious from the CK−TSAC structure that a large modifying agent such as DTNB cannot be readily accommodated in the presence of the substrate creatine. Taken together, the crystallographic and biochemical data are consistent with a model in which the binding of the transition-state complex to one monomer affects the binding affinities in the second monomer of the dimer. Biologically, the negative cooperativity could have the advantage of promoting the release of nucleotide product ADP or ATP after catalysis has occurred. Since either the binding of the bisubstrate complex or the formation of the transition state coincides with closing of the loops (residues 60−70 and 323−332, vide supra), a reasonable structural mechanism for the negative cooperativity would physically link loop closing in the two monomers across the dimer

interface. Although the structural mechanism is not yet clear, it seems that occupancy by the transition state in one monomer directly stabilizes the open form in the second monomer of the dimer.

REFERENCES

1. Wallimann, T., Wyss, M., Brdiczka, D., Nicolay, K., and Eppenberger, H. M. (1992) *Biochem. J. 281* (Part 1), 21−40.
2. Wyss, M., Smeitink, J., Wevers, R. A., and Wallimann, T. (1992) *Biochim. Biophys. Acta 1102*, 119−166.
3. Ellington, W. R. (2001) *Annu. Rev. Physiol. 63*, 289−325.
4. Kenyon, G. L., and Reed, G. H. (1983) *Adv. Enzymol. Relat. Areas Mol. Biol. 54*, 367−426.
5. Furter, R., Furter-Graves, E. M., and Wallimann, T. (1993) *Biochemistry 32*, 7022−7029.
6. Chen, L. H., Borders, C. L., Jr., Vasquez, J. R., and Kenyon, G. L. (1996) *Biochemistry 35*, 7895−7902.
7. Eder, M., Stolz, M., Wallimann, T., and Schlattner, U. (2000) *J. Biol. Chem. 275*, 27094−27099.
8. Cantwell, J. S., Novak, W. R., Wang, P. F., McLeish, M. J., Kenyon, G. L., and Babbitt, P. C. (2001) *Biochemistry 40*, 3056−3061.
9. Hansen, D. E., and Knowles, J. R. (1981) *J. Biol. Chem. 256*, 5967−5969.
10. Rao, J. K., Bujacz, G., and Wlodawer, A. (1998) *FEBS Lett. 439*, 133−137.
11. Eder, M., Schlattner, U., Becker, A., Wallimann, T., Kabsch, W., and Fritz-Wolf, K. (1999) *Protein Sci. 8*, 2258−2269.
12. Eder, M., Fritz-Wolf, K., Kabsch, W., Wallimann, T., and Schlattner, U. (2000) *Proteins 39*, 216−225.
13. Shen, Y. Q., Tang, L., Zhou, H. M., and Lin, Z. J. (2001) *Acta Crystallogr. D57*, 1196−1200.
14. Tisi, D., Bax, B., and Loew, A. (2001) *Acta Crystallogr. D57*, 187−193.
15. Zhou, G., Somasundaram, T., Blanc, E., Parthasarathy, G., Ellington, W. R., and Chapman, M. S. (1998) *Proc. Natl. Acad. Sci. U.S.A. 95*, 8449−8454.
16. Forstner, M., Muller, A., Stolz, M., and Wallimann, T. (1997) *Protein Sci. 6*, 331−339.
17. Forstner, M., Kriechbaum, M., Laggner, P., and Wallimann, T. (1998) *Biophys. J. 75*, 1016−1023.
18. Milner-White, E. J., and Watts, D. C. (1971) *Biochem. J. 122*, 727−740.
19. Wang, P. F., Novak, W. R. P., Cantwell, J. S., Babbitt, P. C., McLeish, M. J., and Kenyon, G. L. (2002) *Protein Expression Purif. 26*, 89−95.
20. Gallagher, S. R. (2002) *Current Protocols in Protein Science Online Unit 10.3*, John Wiley & Sons, Inc.: New York.
21. Milner-White, E. J., and Kelly, I. D. (1976) *Biochem. J. 157*, 23−31.
22. Wang, Z. X., Preiss, B., and Tsou, C. L. (1988) *Biochemistry 27*, 5095−5100.
23. Jancarik, J., and Kim, S. H. (1991) *J. Appl. Crystallogr. 24*, 409−411.
24. Otwinowski, Z., and Minor, W. (1997) *Methods Enzymol. 276*, 307−326.
25. Matthews, B. W. (1985) *Methods Enzymol. 114*, 176−187.
26. Navaza, J. (2001) *Acta Crystallogr. D57*, 1367−1372.
27. Brunger, A. T., Kuriyan, J., and Karplus, M. (1987) *Science 235*, 458−460.
28. Jones, T. A., Zou, J.-Y., Cowan, S. W., and Kjeldgaard, M. (1991) *Acta Crystallogr. A47*, 110−119.
29. Laskowski, R. A., MacArthur, M. W., Moss, D. S., and Thornton, J. M. (1993) *J. Appl. Crystallogr. 26*, 283−291.
30. Milner-White, E. J., and Watts, D. C. (1971) *Biochem. J. 122*, 727−740.
31. Reed, G. H., and McLaughlin, A. C. (1973) *Ann. N.Y. Acad. Sci. 222*, 118−129.
32. Fritz-Wolf, K., Schnyder, T., Wallimann, T., and Kabsch, W. (1996) *Nature 381*, 341−345.
33. Rosevear, P. R., Desmeules, P., Kenyon, G. L., and Mildvan, A. S. (1981) *Biochemistry 20*, 6155−6164.
34. Buechter, D. D., Medzihradszky, K. F., Burlingame, A. L., and Kenyon, G. L. (1992) *J. Biol. Chem. 267*, 2173−2178.
35. Vasak, M., Nagayama, K., Wuthrich, K., Mertens, M. L., and Kagi, J. H. (1979) *Biochemistry 18*, 5050−5055.
36. Leyh, T. S., Goodhart, P. J., Nguyen, A. C., Kenyon, G. L., and Reed, G. H. (1985) *Biochemistry 24*, 308−316.
37. Leyh, T. S., Sammons, R. D., Frey, P. A., and Reed, G. H. (1982) *J. Biol. Chem. 257*, 15047−15053.
38. Reed, G. H., and Leyh, T. S. (1980) *Biochemistry 19*, 5472−5480.
39. Herschlag, D., and Jencks, W. P. (1987) *J. Am. Chem. Soc. 109*, 4665−4674.
40. Struve, G. E., Gazzola, C., and Kenyon, G. L. (1977) *J. Org. Chem. 42*, 4035−4040.
41. Phillips, G. N., Thomas, J. W., Annesley, T. M., and Quiocho, F. A. (1979) *J. Am. Chem. Soc. 101*, 7120−7121.
42. McLaughlin, A. C., Cohn, M., and Kenyon, G. L. (1972) *J. Biol. Chem. 247*, 4382−4388.
43. Wang, P. F., McLeish, M. J., Kneen, M. M., Lee, G., and Kenyon, G. L. (2001) *Biochemistry 40*, 11698−11705.
44. Borders, C. L., Jr., Snider, M. J., Wolfenden, R., and Edmiston, P. L. (2002) *Biochemistry 41*, 6995−7000.
45. Mourad-Terzian, T., Steghens, J. P., Min, K. L., Collombel, C., and Bozon, D. (2000) *FEBS Lett. 475*, 22−26.
46. Price, N. C., and Hunter, M. G. (1976) *Biochim. Biophys. Acta 445*, 364−376.
47. Wang, Z. X., and Pan, X. M. (1996) *FEBS Lett. 388*, 73−75.

BI026655P